Chapter 20
Negative Electrodes in Lithium Systems

20.1 Introduction

A great deal of attention is currently being given to the development and use of batteries in which lithium plays an important role. Looked at very simply, there are two major reasons for this. One is that lithium is a very electropositive element, and its employment in electrochemical cells can lead to larger voltages than are possible with the other, less electropositive alkali metals. The second positive aspect of lithium systems is the possibility of major reductions in weight, at least partly due to the light weight of elemental lithium and many of its alloys and compounds.

Although there are now a number of lithium-based batteries available commercially, there is still a large amount of research and development effort under way. There are two general targets, the achievement of significant improvements in performance and safety, and a great reduction in costs. Since this technology has not matured and stabilized, the discussion here focuses upon phenomena and components, rather than complete systems. This chapter deals with negative electrodes in lithium systems. Positive electrode phenomena and materials are treated in the next chapter.

Early work on the commercial development of rechargeable lithium batteries to operate at or near ambient temperatures involved the use of elemental lithium as the negative electrode reactant. As discussed below, this leads to significant problems. Negative electrodes currently employed on the negative side of lithium cells involving a solid solution of lithium in one of the forms of carbon.

Lithium cells that operate at temperatures above the melting point of lithium must necessarily use alloys instead of elemental lithium. These are generally binary or ternary metallic phases.

There is also increasing current interest in the possibility of the use of metallic alloys instead of carbons at ambient temperatures, with the goal of reducing the electrode volume, as well as achieving significantly increased capacity.

R.A. Huggins, *Energy Storage*, DOI 10.1007/978-3-319-21239-5_20

There are differences in principle between the behavior of elemental and binary phase materials as electrodes. It is the purpose of this chapter to elucidate these principles, as well as to present some examples. Ternary systems are discussed elsewhere.

20.2 Elemental Lithium Electrodes

It is obvious that elemental lithium has the lowest potential, as well as the lowest weight per unit charge, of any possible lithium reservoir material in an electrochemical cell. Materials with lower lithium activities have higher potentials, leading to lower cell voltages, and they also carry along extra elements as dead weight.

There are problems with the use of elemental lithium, however. These are due to phenomena that occur during the recharging of all electrodes composed of simple metallic elements. In the particular case of lithium, however, this is not just a matter of increasing electrode impedance and reduced capacity, as are typically found with other electrode materials. In addition, severe safety problems can ensue. Some of these phenomena will be discussed in the following sections.

In the case of an electrochemical cell in which an elemental metal serves as the negative electrode the process of recharging may seem to be very simple, for it merely involves the electrodeposition of the metal from the electrolyte onto the surface of the electrode. This is not the case, however.

In order to achieve good rechargeability, a consistent geometry must be maintained on both the macroscopic and microscopic scales. Both electrical disconnection of the electroactive species and electronic short circuits must also be avoided. In addition, thermal runaway must not occur.

Phenomena related to the inherent microstructural and macrostructural instability of a growth interface and related thermal problems will now be briefly reviewed.

20.2.1 Deposition at Unwanted Locations

In the absence of a significant nucleation barrier, deposition will tend to occur anywhere at which the electric potential is such that the element's chemical potential is at, or above, that corresponding to unit activity. This means that electrodeposition may take place upon current collectors and other parts of an electrochemical cell that are at the same electrical potential as the negative electrode, as well as upon the electrode structure where it is actually desired. This was a significant problem during the period in which attempts were being made to use pure (molten) lithium as the negative electrode in high-temperature molten halide salt electrolyte cells. Another problem with these high-temperature cells was the fact that alkali metals dissolve in their halides at elevated temperatures. This leads to electronic conduction and self-discharge.

20.2.2 Shape Change

Another difficulty is the *shape change* phenomenon, in which the location of the electrodeposit is not the same as that where the discharge (deplating) process took place. Thus, upon cycling the electrode metal gets preferentially transferred to new locations. For the most part, this is a problem of current distribution and hydrodynamics, rather than being a materials issue. Therefore, it will not be discussed further here.

20.2.3 Dendrites

An additional type of problem relates to the inherent instability of a flat interface on a microscopic scale during electrodeposition, even in the case of a chemically clean surface. It has been shown that there can be an electrochemical analog of the constitutional supercooling that occurs ahead of a growth interface during thermally-driven solidification [1].

This will be the case if the current density is such that solute depletion in the electrolyte near the electrode surface causes the local gradient of the element's chemical potential in the electrolyte immediately adjacent to the solid surface to be positive. Under such a condition there will be a tendency for any protuberance upon the surface to grow at a faster rate than the rest of the interface. This leads to exaggerated surface roughness, and eventually to the formation of either dendrites or filaments. In more extreme cases, it leads to the nucleation of solid particles in the liquid electrolyte ahead of the growing solid interface.

This is also related to the inverse phenomenon, the formation of a flat interface during electropolishing, as well as the problem of morphology development during the growth of an oxide layer upon a solid solution alloy [2, 3]. Another analogous situation is present during the crystallization of the solute phase from liquid metal solutions.

The protuberances upon a clean growing interface can grow far ahead of the general interface, often developing into dendrites. A general characteristic of dendrites is a tree-and-branches type of morphology, which has very distinct geometric and crystallographic characteristics, due to the orientation dependence of either the surface energy or the growth velocity.

20.2.4 Filamentary Growth

A different phenomenon that is often mistakenly confused with dendrite formation is the result of the presence of a reaction product layer upon the growth interface if the electrode and electrolyte are not stable in the presence of each other.

The properties of these layers can have an important effect upon the behavior of the electrode. In some cases they may be useful solid electrolytes, and allow electrodeposition by ionic transport through them. Such layers upon negative electrodes in lithium systems have been given the name *SEI*, and will be discussed in a later chapter. But in other cases reaction product layers may be ionically blocking, and thus significantly increase the interfacial impedance.

Interfacial layers often have defects in their structure that can lead to local variations in their properties. Regions of reduced impedance can cause the formation of deleterious filamentary growths upon recharge of the electrode. This is an endemic problem with the use of organic solvent electrolytes in contact with lithium electrodes at ambient temperatures.

When a protrusion grows ahead of the main interface the protective reaction product layer will typically be locally less thick. This means that the local impedance to the passage of ionic current is reduced, resulting in a higher current density and more rapid growth in that location. This behavior can be exaggerated if the blocking layer is somewhat soluble in the electrolyte, with a greater solubility at elevated temperatures. When this is the case, the higher local current leads to a higher local temperature, and a greater solubility. The result is then a locally thinner blocking layer, and an even higher local current.

Furthermore, the current distribution near the tip of a protrusion that is well ahead of the main interface develops a 3-dimensional character, leading to even faster growth than the main electrode surface, where the mass transport is essentially 1-dimensional. Especially in relatively low concentration solutions, this leads to a runaway type of process, so that the protrusions consume most of the solute, and grow farther and farther ahead of the main, or bulk, interface.

This phenomenon can result in the metal deposit having a hairy or spongy character. During a subsequent discharge step, the protrusions often get disconnected from the underlying metal, so that they cannot participate in the electrochemical reaction, and the rechargeable capacity of the electrode is reduced.

This unstable growth is a major problem with the rechargeability of elementary negative electrodes in a number of electrochemical systems, and constitutes an important limitation upon the development of rechargeable lithium batteries using elemental lithium as the negative electrode reactant.

20.2.5 Thermal Runaway

The organic solvent electrolytes that are typically used in lithium batteries are not stable in the presence of high lithium activities. This is a common problem when using elemental lithium negative electrodes in contact with electrolytes containing organic cationic groups, regardless of whether the electrolyte is an organic liquid or a polymer [4].

They react with lithium and form either crystalline or amorphous product layers upon the surface of the electrode structure. These reactions are exothermic and

cause local heating. Experiments using an *accelerating rate calorimeter* have shown that this problem increases dramatically as cells are cycled, presumably due to an increase in the surface area of the lithium due to morphological instability during repetitive recharging [5]. This is a fundamental difficulty with elemental lithium electrodes, and has led to serious safety problems.

The exothermic formation of reaction product films also occurs when carbon or alloy electrodes are used that operate at potentials at which the electrolyte reacts with lithium. However, if their morphology is constant the surface area does not change substantially, so that it can lead to heating, but typically does not lead to thermal runaway at the negative electrode.

20.3 Alternatives to the Use of Elemental Lithium

Because of these safety and cycle life problems with the use of elemental lithium, essentially all commercial rechargeable lithium batteries now use lithium–carbon alloys as negative electrode reactants today.

A considerable amount of research attention is now also being given to the possibility of the use of metallic lithium alloys instead of the carbons, because of the expectation that this may lead to significant increases in capacity. The large volume changes that accompany increased capacity present a significant problem, however. These matters, as well as the possibility of the use of novel micro- or nano-structures to alleviate this difficulty, are briefly discussed later in this chapter.

20.4 Lithium–Carbon Alloys

20.4.1 Introduction

Lithium–carbons are currently used as the negative electrode reactant in the very common small rechargeable lithium batteries used in consumer electronic devices. As will be seen in this chapter, a wide range of structures, and therefore of properties, is possible in this family, depending upon how the carbon is produced. The choices made by the different manufacturers are not all the same. Several good reviews of the materials science aspects of this topic can be found in the literature [6, 7].

The crystal structure of pure graphite is shown schematically in Fig. 20.1. It consists of parallel sheets containing interconnected hexagons of carbon, called *graphene* layers or sheets. They are stacked with alternate layers on top of one another. This is described as A-B-A-B-A stacking.

Graphite is amphoteric, and either cations or anions can be inserted into it between the graphene layers. When cations are inserted, the host graphite structure

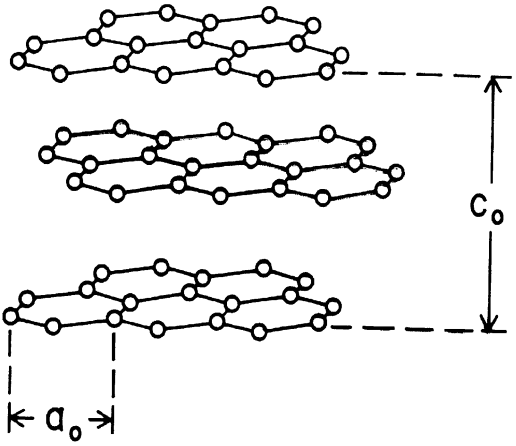

Fig. 20.1 Model of a portion of the crystal structure of graphite

takes on a negative charge. Cation examples are Li^+, K^+, Rb^+, Cs^+. When anions are inserted, the host graphite structure takes on a positive charge, and anion examples are Br^-, SO_4^{2-}, or SbF_6^-.

The insertion of alkali metals into carbon was first demonstrated in 1926 [8], and the chemical synthesis of lithium–carbons was demonstrated in 1955 [9]. X-ray photoemission spectroscopy experiments showed that the inserted lithium gives up its electron to the carbon, and thus the structure can be viewed as Li^+ ions contained between the carbon layers of the graphite structure [10]. A general review of the early work on the insertion of species into graphite can be found in [11].

Insertion often is found to occur in "stages," with nonrandom filling of positions between the layers of the host crystal structure. This ordering can occur in individual layers, and also in the filling of the stack of layers.

The possibility of the use of graphite as a reactant in the negative electrode of electrochemical cells containing lithium was first investigated than some 30 years ago [12]. The experiments were, however, unsuccessful. Swelling and defoliation occurred due to co-intercalation of species from the organic solvent electrolytes that were used at that time.

This problem has been subsequently solved by the use of other liquid electrolytes.

Attention was again brought to this possibility by a conference paper that was presented in 1983 [13] that showed that lithium can be reversibly inserted into graphite at room temperatures when using a polymeric electrolyte. Although not publicly known at that time, two patents relating to the use of the insertion of lithium into graphite as a reversible negative electrode in lithium systems, at both elevated [14] and ambient [15] temperatures, had already been submitted by Bell Laboratories. Royalties paid for the use of these patents have become very large.

This situation changed abruptly as the result of the successful development by SONY in 1990 of commercial rechargeable batteries containing negative electrodes based upon materials of this family and their commercial introduction as the power source in camcorders [16, 17].

There has been a large amount of work on the understanding and development of graphites and related carbon-containing materials for use as negative electrode materials in lithium batteries since that time.

Lithium–carbon materials are, in principle, no different from other lithium-containing metallic alloys. However, since this topic is treated in more detail later, only a few points that specifically relate to carbonaceous materials are discussed here.

One is that the behavior of these materials is very dependent upon the details of both the nanostructure and the microstructure. Therefore, the composition and the thermal and mechanical treatment of the electrode materials all play important roles in determining the resulting thermodynamic and kinetic properties. Materials with a more graphitic structure have properties that are much different from those with less well-organized structures. The materials that are used by the various commercial producers are not all the same, as they reflect the different choices that they have made for their specific products. However, the major producers of small consumer lithium batteries generally now use relatively graphitic carbons.

An important consideration in the use of carbonaceous materials as negative electrodes in lithium cells is the common observation of a considerable loss of capacity during the first charge-discharge cycle due to irreversible lithium absorption into the structure, as will be seen later. This has the distinct disadvantage that it requires that an additional amount of lithium be initially present in the cell. If this irreversible lithium is supplied from the positive electrode, an extra amount of the positive electrode reactant material must be put into the cell during its fabrication. As the positive electrode reactant materials often have relatively low specific capacities, e.g., around 140 mAh/g, this irreversible capacity in the negative electrode leads to a requirement for an appreciable amount of extra reactant material weight and volume in the total cell.

20.4.2 Ideal Structure of Graphite Saturated with Lithium

Lithium can be inserted into the graphite structure up to a maximum concentration of one Li per six carbons, or LiC_6. One of the major influences of the presence of lithium is the graphite crystal structure is that the stacking of graphene layers is changed by the insertion of lithium. It changes from A-B-A-B-A stacking to A-A-A-A-A stacking. This is illustrated schematically in Fig. 20.2.

The distribution of lithium ions within the gallery space between the graphene layers is illustrated schematically in Fig. 20.3.

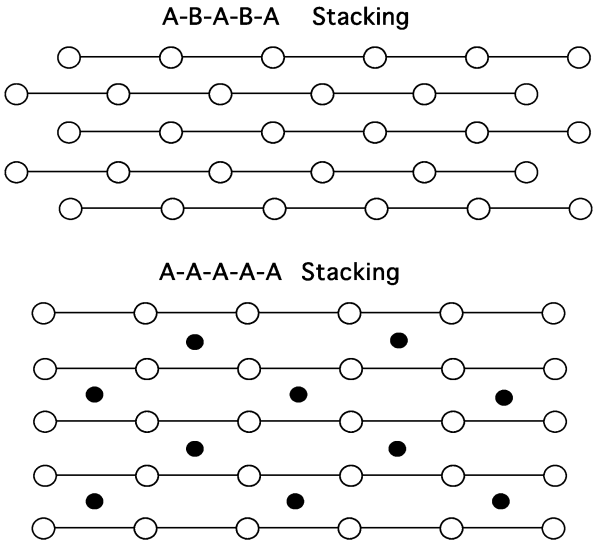

Fig. 20.2 Difference between the A-B-A-B-A and A-A-A-A-A stacking of the graphene layers when lithium is inserted. The *black circles* are the lithium ions

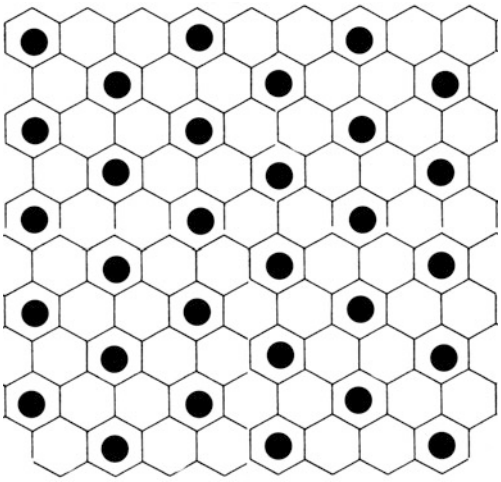

Fig. 20.3 Schematic representation of the lithium distribution in the gallery space in relation to the carbon hexagonal network in the adjacent graphene layers

20.4.3 Variations in the Structure of Graphite

There is actually a wide range of lithium–carbon structures, and most such materials do not actually have the ideal graphite structure. The ones that are closest are made

synthetically by vapor transport, and are called highly ordered pyrolytic graphite (HOPG). This is a slow and very expensive process. The graphites that are used commercially range from natural graphite to materials formed by the pyrolysis of various polymer or hydrocarbon precursors. They are often divided into two general types, designated as *soft*, *or graphitizing*, *carbons*, and *hard carbons* [18].

At modest temperatures and pressures there is a strong tendency for carbon atoms to be arranged in a planar graphene-type configuration, rather than a 3-dimensional structure such as that in diamond.

Soft carbons are generally produced by the pyrolysis of liquid materials such as petroleum pitch, which is the residue from the distillation of petroleum fractions.

The carbon atoms in their structure are initially arranged in small graphene-type groups, but there is generally a significant amount of imperfection in their two-dimensional honeycomb networks, as well as randomness in the way that the layers are vertically stacked upon each other. In addition there is little coordination in the rotational orientation of nearby graphene layers. The term *turbostratic* is generally used to describe this general type of 3-dimensional disorder in carbons [18].

The three types of initial disorder, in-plane defects, inter-plane stacking defects, and rotational misorientation, gradually become healed as the temperature is raised: the first two earlier than the rotational disorder between adjacent layers, for that requires more thermal energy.

The microstructure of such materials that have been heated to intermediate temperatures is shown schematically in Fig. 20.4.

At this intermediate stage, the structure contains many small three-dimensional subgrains.

In addition to containing some internal imperfections, they differ from their neighbors in both vertical and horizontal orientations. They are separated by subgrain walls (boundaries) that have surface energy. This subgrain wall surface energy gradually gets reduced as the individual subgrains grow in size and the overall graphitic structure becomes more perfect.

The *hard carbons*, that are typically produced by the pyrolysis of solid materials, such as chars or glassy carbon, initially have a significant amount of initial cross-linking, related to the structure of their precursors. In addition, they can have a

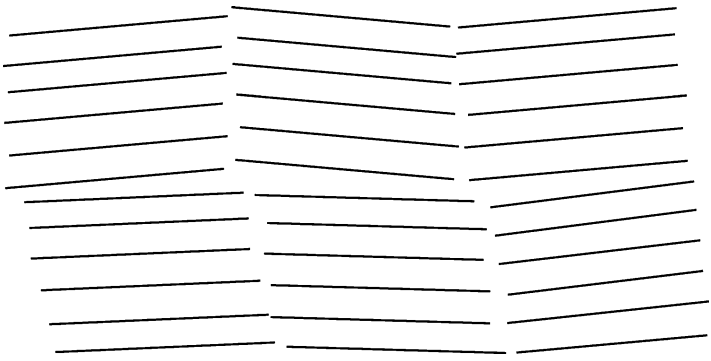

Fig. 20.4 Schematic drawing of the microstructure of graphite after heating to intermediate temperatures

substantial amount of nano-porosity. As a result, it is more difficult to make these structural rearrangements and turbostratic disorder is more persistent. The result is the requirement for more thermal energy, i.e., higher temperatures.

The structure that results from the pyrolysis of carbonaceous precursors depends greatly upon the maximum temperature that is reached. Heating initially amorphous, or *soft*, carbons to the range of 1,000–2,000 °C produces microstructures in which graphene sheets form and begin to grow, with diameters up to about 15 nm, and they become assembled into small stacks of 50–100 sheets. These subgrains initially have a turbostratic arrangement, but their alignment into larger ordered, i.e., graphitic, regions gradually takes place as the temperature is increased from 2000 to 3000 °C.

20.4.4 Structural Aspects of Lithium Insertion into Graphitic Carbons

One of the important features in the interaction of lithium with graphitic materials is the phenomenon of *staging*. Lithium that enters the graphite structure is not distributed uniformly between all the graphene layers at ambient temperatures. Instead, it resides in certain interlayer *galleries*, but not others, depending upon the total amount of lithium present.

The distribution is described by the number of graphene layers between those that have the lithium guest ions present. A stage 1 structure has lithium between all of the graphene layers, a stage 2 structure has an empty gallery between each occupied gallery, and a stage 4 structure has four graphene layers between each gallery containing lithium. This is discussed a bit more later in this chapter. This is obviously a simplification, for in any real material there will be regions with predominately one structure, and other regions with another.

The phenomenon of nonrandom gallery occupation is found in a number of other materials, and can be attributed to a catalytic effect, in which the ions that initially enter a gallery pry open the van der Waals-bonded interlayer space, making it easier for following ions to enter.

However, the situation is a bit more complicated, for there must be communication between nearby galleries in order for the structure to adopt the ordered stage structure. This is related to the inter-tunnel communication in the *hollandite* structure described in Chap. 13, but will not be further discussed here.

20.4.5 Electrochemical Behavior of Lithium in Graphite

The electrochemical behavior of lithium in carbon materials is highly variable, depending upon the details of the graphitic structure. Materials with a more perfect

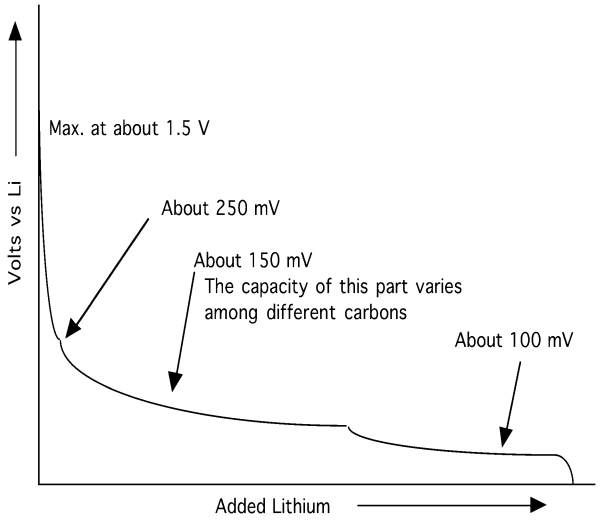

Fig. 20.5 Typical discharge curve of a lithium battery negative electrode

graphitic structure react with lithium at more negative potentials, whereas those with less well organized structures typically operate over much wider potential ranges, resulting in cell voltages that are both lower and more state-of-charge dependent.

In a number of cases, the carbons that are used in commercial batteries have been heated to temperatures over bout 2400 °C, where they become quite well graphitized. Capacities typically range from 300 to 350 mAh/g, whereas the maximum theoretical value (for LiC_6) is 372 mAh/g.

A typical discharge curve under operating conditions, with currents as large as 2–4 mA/cm^2, is shown in Fig. 20.5.

This behavior is not far from what is found under near equilibrium conditions, as shown in Fig. 20.6. It can be seen that there is a difference between the data during charge, when lithium is being added, and discharge, when lithium is being deleted. This displacement (hysteresis) between the charge and discharge curves is at least partly due to the mechanical energy involved in the structural changes.

It can be seen that these data show plateaus, indicating the presence of three ranges of composition within which reconstitution reactions take place. As the composition changes along these plateaus the relative amounts of material with the two end compositions varies. This means that there will be regions, or domains, where the graphene layer stacking is of one type, and regions in which it has the other. The relative volumes of these two domains varies as the overall composition traverses these *two phase regions*. The differences in stacking results in differences in interlayer spacing, and therefore considerable amount of distortion of the structure. Such a model was presented some time ago by Daumas and Herold [20].

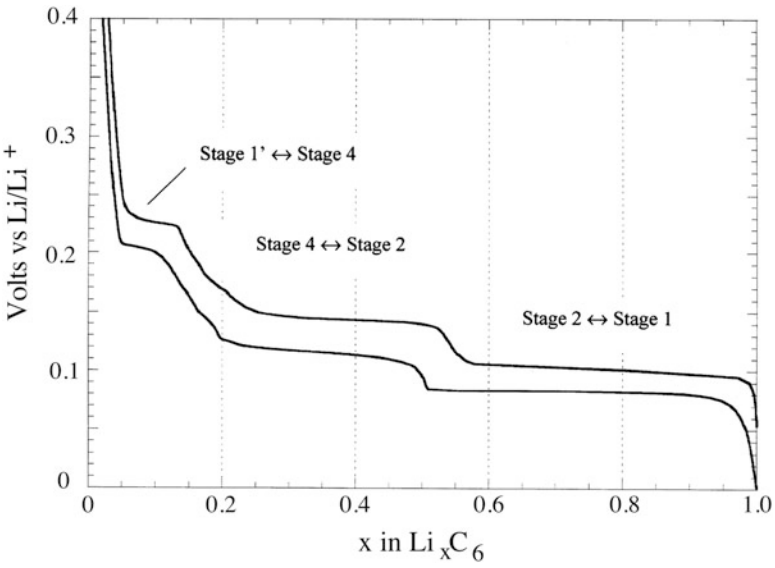

Fig. 20.6 Potential versus composition during lithiation and delithiation of a graphite electrode at the C/50 rate at ambient temperature. After [19]

20.4.6 Electrochemical Behavior of Lithium in Amorphous Carbons

The electrochemical behavior is quite different when the carbon has not been heated so high, and the structure is not so well ordered. There is a wide range of possible sites in which the lithium can reside, with different local structures, and therefore different energies. The result is that the potential varies gradually, rather than showing the steps characteristic of more ordered structures. This is shown in Fig. 20.7. It can be seen that, in addition to varying with the state of charge, the potential is significantly greater than is found in the graphitic materials. This means that the cell voltages are correspondingly lower.

It can be seen that there was some capacity loss on the first cycle. The capacity upon the first charging (that is not useful) was greater than the capacity in the subsequent discharge cycle. The source of this phenomenon is not yet understood, but there must be some lithium that is *trapped* in the structure and does not come out during discharge. Because of this extra (useless) capacity during the initially charging of this negative electrode it is necessary to put extra capacity in the positive electrode. This is unfortunate, for the specific capacity of the positive electrodes in such systems is less than that in the negative electrodes. As a result, a significant amount of extra weight and volume is necessary.

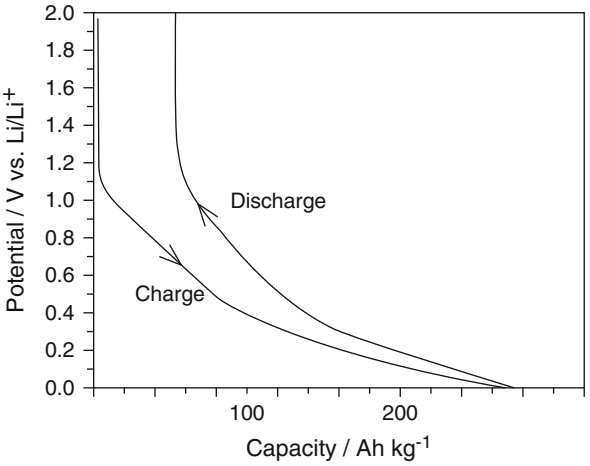

Fig. 20.7 Typical data for the reaction of lithium with an amorphous carbon

20.4.7 Lithium in Hydrogen-Containing Carbons

It is often found that there is a considerable amount of hydrogen initially present in various carbons, depending upon the nature of the precursor. This gradually disappears as the temperature is raised.

If the precursor is heated to only 500–700 °C, there is still a lot of hydrogen present in the structure. It has been found experimentally that this can lead to a very large capacity for lithium that is proportional to the amount of hydrogen present [21–23]. There is a loss in this capacity upon cycling, perhaps due to the gradual loss of hydrogen in the structure.

The large capacity may be due to lithium binding to hydrogen-terminated edges of small graphene fragments. The local configuration would then be analogous to that in the organolithium molecule $C_2H_2L_2$. This is consistent with the experimental observation of the dependence of the lithium capacity upon the amount of hydrogen present. This would also result in a change in the local bonding of the host carbon atom from sp^2 to sp^3.

In addition to a large capacity, experiments have shown a very large hysteresis with these materials [23]. Hysteresis is generally considered to be a disadvantage, as the discharge potential is raised, reducing the cell voltage.

Hysteresis is characteristic of reactions that involve a lot of mechanical energy as the result of shape and volume changes. However, in this case it is more likely due to the energy involved in the change of the bonding of the nearby carbon atoms [23].

The results of experiments performed on one example of a hydrogen-containing material are shown in Fig. 20.8. It can be seen that there was a very large capacity loss on the first cycle. The capacity upon the first charging (that is not useful) was much greater than the capacities in subsequent cycles. As mentioned above, this extra lithium must be supplied by the positive electrode. The

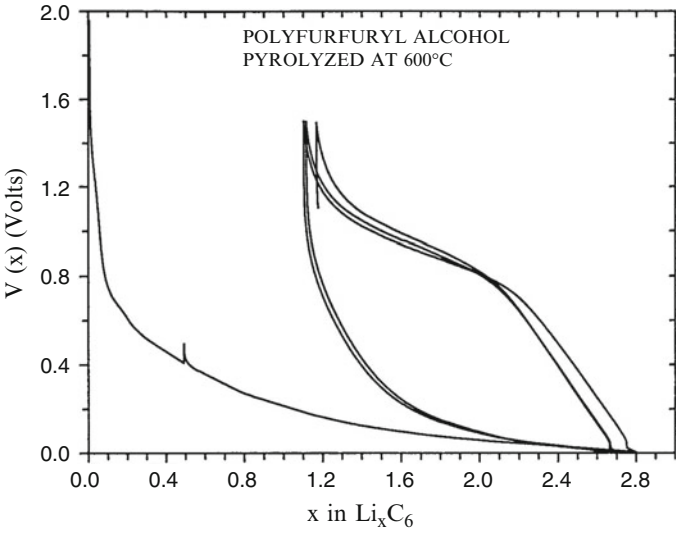

Fig. 20.8 Charge–discharge curves for a material containing hydrogen. After [7]

source of this phenomenon is not yet understood, but there must be a lot of lithium that is *trapped* in the structure and does not come out during the first, and subsequent, discharges.

20.5 Metallic Lithium Alloys

20.5.1 Introduction

Attention has been given to the use of lithium alloys as an alternative to elemental lithium for some time. Groups working on batteries with molten salt electrolytes that operate at temperatures of 400–450 °C, well above the melting point of lithium, were especially interested in this possibility. Two major directions evolved. One involved the use of lithium-aluminum alloys [24, 25], whereas another was concerned with lithium–silicon alloys [26–28].

Whereas this approach can avoid the problems related to lithium melting, as well as the others mentioned above, there are always at least two disadvantages related to the use of alloys. Because they reduce the activity of the lithium they necessarily reduce the cell voltage. In addition, the presence of additional species that are not directly involved in the electrochemical reaction always brings additional weight, and often volume. Thus the maximum theoretical values of the specific energy are always reduced compared to what might be attained with pure lithium. The energy density is also often reduced. But lithium has a large specific volume, so that this is not always the case.

In practical cases, however, the excess weight and volume due to the use of alloys may not be very far from those required with pure lithium electrodes, for it is generally necessary to have a large amount of excess lithium in rechargeable cells in order to make up for the capacity loss related to the dendrite or filament growth problem upon cycling.

Lithium alloys have been used for a number of years in the high temperature "thermal batteries" that are produced commercially for military purposes. These devices are designed to be stored for long times at ambient temperatures before use, where their self-discharge kinetic behavior is very slow. They must be heated to elevated temperatures when their energy output is desired. An example is the Li alloy/FeS_2 battery system that employs a chloride molten salt electrolyte. In order to operate, the temperature must be raised to over the melting point of the electrolyte. This type of cell typically uses either Li–Si or Li–Al alloys in the negative electrode.

The first use of lithium alloys as negative electrodes in commercial batteries to operate at ambient temperatures was the employment of Wood's metal alloys in lithium-conducting button type cells by Matsushita in Japan. Development work on the use of these alloys started in 1983 [29], and they became commercially available somewhat later.

20.5.2 Equilibrium Thermodynamic Properties of Binary Lithium Alloys

Useful starting points when considering lithium alloys as electrode reactants are their phase diagrams and equilibrium thermodynamic properties. In some cases this information is available, so that predictions can be made of their potentials and capacities. In other cases, experimental measurements are required. Relevant principles were discussed in earlier chapters, and will not be repeated here.

Elevated temperature data for a number of phases in the Li–Al, Li–Bi, Li–Cd, Li–Ga, Li–In, Li–Pb, Li–Sb, Li–Si, and Li–Sn binary lithium alloy systems, made using a LiCl–KCl molten salt electrolyte, are listed in Table 20.1.

20.5.3 Experiments at Ambient Temperature

Experiments have also been performed to determine the equilibrium values of the electrochemical potentials and capacities in a smaller number of binary lithium systems at ambient temperatures [30, 31]. Because of slower kinetics at lower temperatures, these experiments took longer to perform. Data are presented in Table 20.2.

Table 20.1 Plateau potentials and composition ranges of a number of binary lithium alloys at 400 °C

Voltage vs Li/Li^+	System	Range of y
0.910	Li_ySb	0–2.0
0.875	Li_ySb	2.0–3.0
0.760	Li_yBi	0.6–1.0
0.750	Li_yBi	1.0–2.82
0.570	Li_ySn	0.57–1.0
0.455	Li_ySn	1.0–2.33
0.430	Li_ySn	2.33–2.5
0.387	Li_ySn	2.5–2.6
0.283	Li_ySn	2.6–3.5
0.170	Li_ySn	3.5–4.4
0.565	Li_yGa	0.15–0.82
0.122	Li_yGa	1.28–1.48
0.09	Li_yGa	1.53–1.93
0.558	Li_yCd	0.12–0.21
0.373	Li_yCd	0.33–0.45
0.058	Li_yCd	1.65–2.33
0.507	Li_yPb	0–1.0
0.375	Li_yPb	1.1–2.67
0.271	Li_yPb	2.67–3.0
0.237	Li_yPb	3.0–3.5
0.089	Li_yPb	3.8–4.4
0.495	Li_yIn	0.22–0.86
0.145	Li_yIn	1.74–1.92
0.080	Li_yIn	2.08–2.67
0.332	Li_ySi	0–2.0
0.283	Li_ySi	2.0–2.67
0.156	Li_ySi	2.67–3.25
0.047	Li_ySi	3.25–4.4
0.300	Li_yAl	0.08–0.9

20.5.4 Liquid Binary Alloys

Although the discussion here has involved solid lithium alloys, similar considerations apply to those based on sodium or other species. In addition, it is not necessary that the active material be solid. The same principles hold for liquids.

An example was discussed in Chap. 3 relating to the so-called sodium–sulfur battery that operates at about 300 °C. In this case, both of the electrodes are liquids, and the electrolyte is a solid sodium ion conductor. This configuration can thus be described as an L/S/L system. It is the inverse of conventional systems with solid electrodes and a liquid electrolyte, S/L/S systems.

Table 20.2 Plateau potentials and composition ranges of lithium alloys at ambient temperatures under equilibrium conditions

Voltage vs. Li/Li^+	System	Range of y
0.956	Li_ySb	1.0–2.0
0.948	Li_ySb	2.0–3.0
0.828	Li_yBi	0–1.0
0.810	Li_yBi	1–3.0
0.680	Li_yCd	0–0.3
0.352	Li_yCd	0.3–0.6
0.055	Li_yCd	1.5–2.9
0.660	Li_ySn	0.4–0.7
0.530	Li_ySn	0.7–2.33
0.485	Li_ySn	2.33–2.63
0.420	Li_ySn	2.6–3.5
0.380	Li_ySn	3.5–4.4
0.601	Li_yPb	0–1.0
0.449	Li_yPb	1.0–3.0
0.374	Li_yPb	3.0–3.2
0.292	Li_yPb	3.2–4.5
0.256	Li_yZn	0.4–0.5
0.219	Li_yZn	0.5–0.67
0.157	Li_yZn	0.67–1.0
0.005	Li_yZn	1.0–1.5

20.5.5 Mixed-Conductor Matrix Electrodes

In order to be able to achieve appreciable macroscopic current densities while maintaining low local microscopic charge and particle flux densities, many battery electrodes that are used in conjunction with liquid electrolytes are produced with porous microstructures containing very fine particles of the solid reactant materials. This high reactant surface area porous structure is permeated with the electrolyte.

This porous fine-particle approach has several characteristic disadvantages, however. Among these are difficulties in producing uniform and reproducible microstructures, and limited mechanical strength when the structure is highly porous. In addition, they often suffer Ostwald ripening, sintering, or other time-dependent changes in both microstructure and properties during cyclic operation.

Furthermore, it is often necessary to have an additional material present in order to improve the electronic transport within an electrode. Various highly dispersed carbons are often used for this purpose.

A quite different approach was introduced some years ago [32–34] in which it was demonstrated that a rather dense solid electrode can be fabricated that has a composite microstructure in which particles of the reactant phase or phases are finely dispersed within a solid electronically-conducting matrix in which the electroactive species is also mobile, i.e., within a mixed conductor. There is

thus a large internal reactant/mixed-conducting matrix interfacial area. The electroactive species is transported through the solid matrix to this interfacial region, where it undergoes the chemical part of the electrode reaction. Since the matrix material is also an electronic conductor, it can also act as the electrode's current collector. The electrochemical part of the reaction takes place on the outer surface of the composite electrode.

When such an electrode is discharged by deletion of the electroactive species, the residual particles of the reactant phase remain as relics in the microstructure. This provides fixed permanent locations for the reaction to take place during following cycles, when the electroactive species again enters the structure. Thus this type of configuration has the additional advantage that it can provide a mechanism for the achievement of true microstructural reversibility.

In order for this concept to be applicable, the matrix and the reactant phases must be thermodynamically stable in contact with each other. One can evaluate this possibility if one has information about the relevant phase diagrams as well as the titration curves of the component binary systems. The stability window of the matrix phase must span the reaction potential of the reactant material. It has been shown that one can evaluate the possibility that these conditions are met from knowledge of the binary titration curves.

Since there is generally a common component, these two binaries can also be treated as a ternary system. Although ternary systems are not explicitly discussed here, it can be simply stated that the two materials must lie at corners of the same constant-potential tie triangle in the relevant isothermal ternary phase diagram in order to not interact. The potential of the tie triangle determines the electrode reaction potential, of course. An additional requirement is that the reactant material must have two phases present in the tie triangle, but the matrix phase only one.

The kinetic requirements for a successful application of this concept are readily understandable. The primary issue is the rate at which the electroactive species can reach the matrix/reactant interfaces. The critical parameter is the chemical diffusion coefficient of the electroactive species in the matrix phase. This can be determined by various techniques, as discussed in later chapters.

The first example that was demonstrated was the use of the phase with the nominal composition $Li_{13}Sn_5$ as the matrix, in conjunction with reactant phases in the lithium-silicon system at temperatures near 400 °C. This is an especially favorable case, due to the very high chemical diffusion coefficient of lithium in the $Li_{13}Sn_5$ phase.

The relation between the potential-composition data for these two systems under equilibrium conditions is shown in Fig. 20.9 [32]. It is seen that the phase $Li_{2.6}Sn$ ($Li_{13}Sn_5$) is stable over a potential range that includes the upper two-phase reconstitution reaction plateau in the lithium–silicon system. Therefore, lithium can react with Si to form the phase $Li_{1.71}Si$ ($Li_{12}Si_7$) inside an all-solid composite electrode containing the $Li_{2.6}Sn$ phase, which acts as a lithium-transporting, but electrochemically inert matrix.

Figure 20.10 shows the relatively small polarization that is observed during the charge and discharge of this electrode, even at relatively high current densities [32].

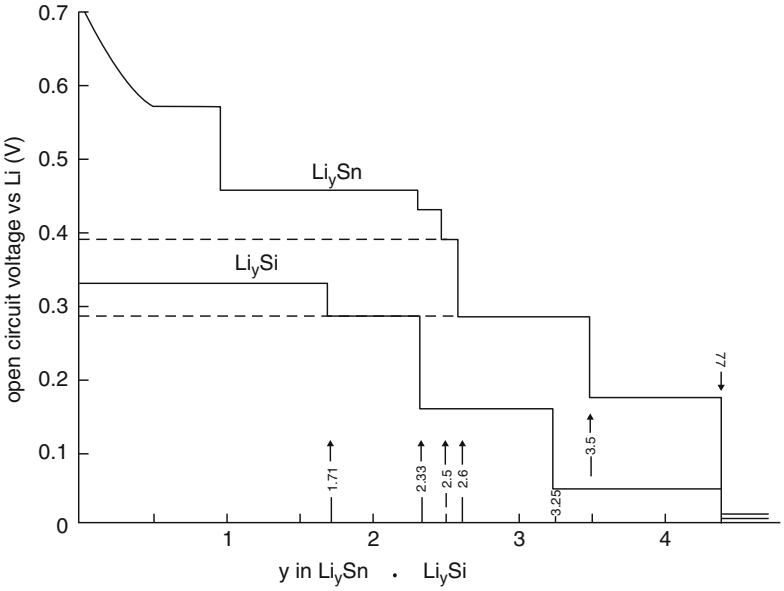

Fig. 20.9 Composition dependence of the potential in the Li–Sn and Li–Si systems. After [32]

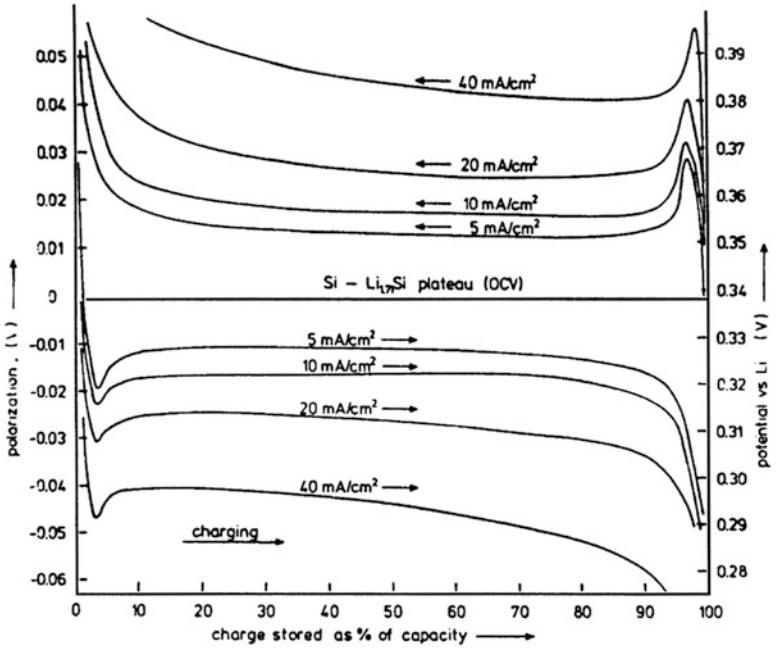

Fig. 20.10 Charge and discharge curves of the Li–Si alloy in the matrix of the electrochemically inert mixed-conducting Li–Sn alloy at different current densities. After [32]

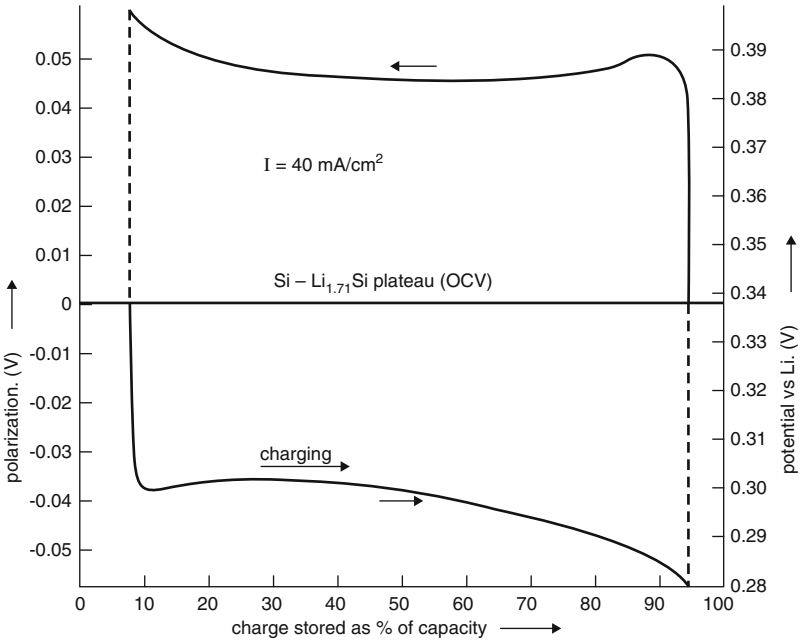

Fig. 20.11 Charge and discharge curves of the Li–Si and Li–Sn composite if the capacity is limited so that the reaction does not go to completion in either direction. There is no large nucleation overshoot in this case. After [32]

It is seen that there is a potential overshoot due to the free energy involved in the nucleation of a new second phase if the reaction goes to completion in each direction. On the other hand, if the composition is not driven quite so far, so that there is some of the reactant phase remaining, this nucleation-related potential overshoot does not appear, as seen in Fig. 20.11 [32].

This concept has also been demonstrated at ambient temperature in the case of the Li–Sn–Cd system [35, 36]. The composition-dependence of the potentials in the two binary systems at ambient temperatures is shown in Fig. 20.12, and the calculated phase stability diagram for this ternary system is shown in Fig. 20.13. It was shown that the phase $Li_{4.4}Sn$, which has fast chemical diffusion for lithium [37], is stable at the potentials of two of the Li–Cd reconstitution reaction plateaus, and therefore can be used as a matrix phase. The behavior of this composite electrode, in which Li reacts with the Cd phases inside of the Li-Sn phase, is shown in Fig. 20.14.

In order to achieve good reversibility, the composite electrode microstructure must have the ability to accommodate any volume changes that might result from the reaction that takes place internally. This can be taken care of by clever microstructural design and alloy fabrication techniques.

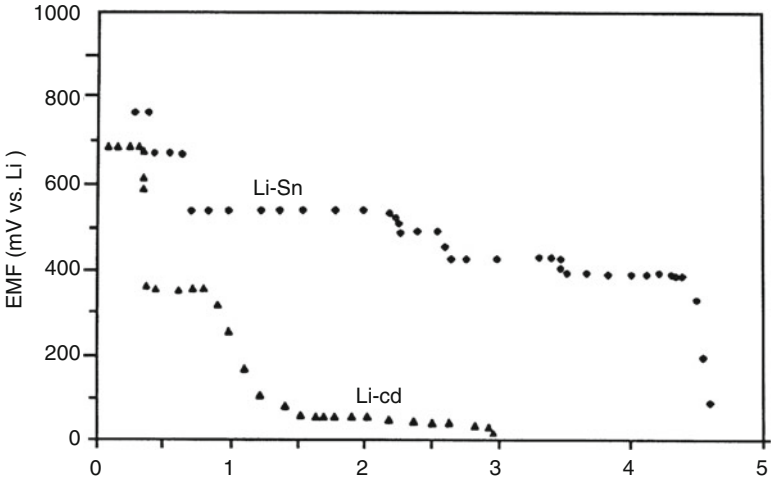

Fig. 20.12 Potential versus composition for Li–Sn and Li–Cd systems at ambient temperature. After [36]

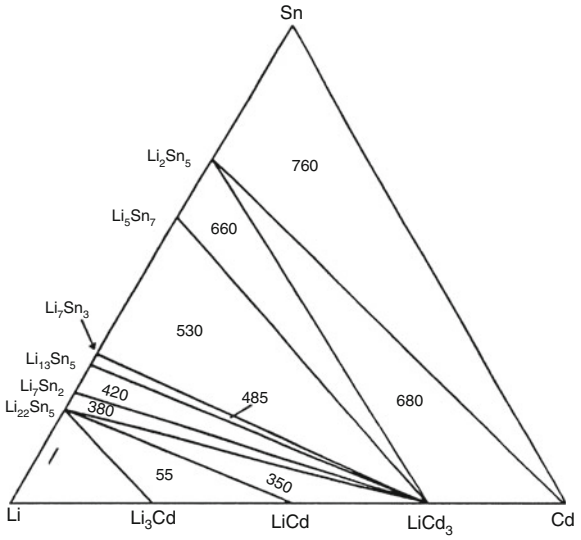

Fig. 20.13 Calculated phase stability diagram for the Li–Cd–Sn system at ambient temperature. *Numbers* are voltages vs. Li. After [36]

20.5.6 Decrepitation

A phenomenon called *decrepitation*, that is also sometimes called *crumbling*, can occur in materials that undergo significant volume changes upon the insertion of guest species. These dimensional changes cause mechanical strain in the microstructure, often resulting in the fracture of particles in an electrode into smaller pieces.

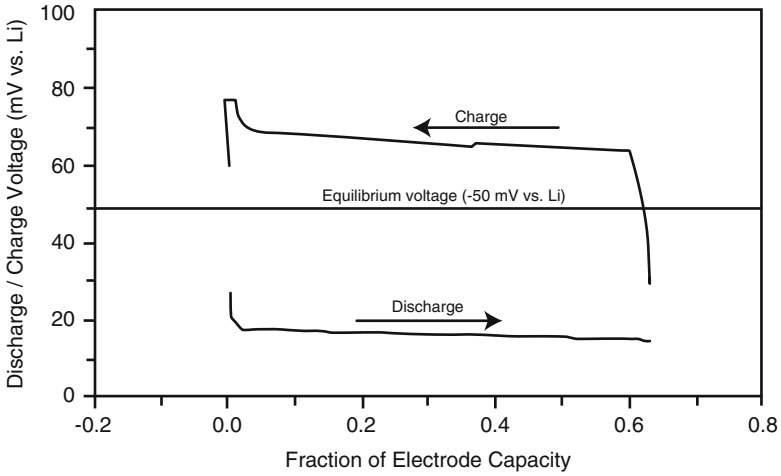

Fig. 20.14 Charge–discharge curve of the Li–Cd system with a fast mixed-conducting phase in the lithium–tin system at ambient temperature. After [37]

This can be a striking, and sometimes disastrous, phenomenon, for it is not specifically related to fine particles, or even to electrochemical systems. As an example, it has been shown that some bulk solid metals can be caused to fracture, and can even be converted into powders by repeated exposure to hydrogen gas if they form metal hydrides under the particular thermodynamic conditions present. This is, of course, different from the hydrogen embrittlement problem in metals with body-centered cubic crystal structures, which involves the segregation of hydrogen to dislocations within the microstructure, influencing their mobility.

Decrepitation is often particularly evident during cycling of electrochemical systems. It can readily result in the loss of electronic contact between reactive constituents in the microstructure and the current collector. As a consequence, the reversible capacity decreases.

This phenomenon has long been recognized in some electrochemical systems in which metal hydrides are employed as negative electrode reactants.

Similar phenomena also occur in lithium systems employing alloy electrodes, some of which undergo very large changes in specific volume if the composition is varied over a wide range in order to achieve a large charge capacity.

Because of its potentially large capacity, a considerable amount of attention has been given recently to the Li–Sn system, which is a fine example of this phenomenon. The phase diagram of the Li–Sn system shows that there are six intermediate phases. The thermodynamic and kinetic properties of the different phases in this system were investigated some time ago at elevated temperatures [37, 38] and also at ambient temperatures [30, 31, 35, 36]. The volume changes that occur in connection with phase changes in this alloy system are large. The phase that forms at the highest lithium concentration, $Li_{4.4}Sn$, has a specific volume that is

283 % of that of pure tin. Thus Li–Sn electrodes swell and shrink, or *breathe*, a lot as lithium is added or deleted.

Observations on metal hydrides that undergo larger volume changes have shown that this process does not continue indefinitely. Instead, it is found that there is a terminal particle size that is characteristic of a particular material. Particles with smaller sizes do not fracture further.

Experiments on lithium alloy electrodes have also shown that the electrochemical cycling behavior is significantly improved if the initial particle size is already very small [39], and it is reasonable to conclude that this is related to the terminal particle size phenomenon.

A theoretical study of the mechanism and the influence of the important parameters related to decrepitation utilized a simple one-dimensional model to calculate the conditions under which fracture will be caused to occur in a two-phase structure due to a specific volume mismatch [40]. This model predicts that there will be a terminal particle size below which further fracture will not occur. The value of this characteristic dimension is material-specific, depending upon two parameters, the magnitude of a strain parameter related to the volume mismatch and the fracture toughness of the lower-specific-volume phase. For the same value of volume mismatch, the tendency to fracture will be reduced and the terminal particle size will be larger the greater the toughness of the material. The results of this model calculation are shown in Fig. 20.15 [40].

The magnitude of the volume change depends upon the amount of lithium that has entered the alloy crystal structure, and is essentially the same for all lithium alloys. This is shown in Fig. 20.16 [41].

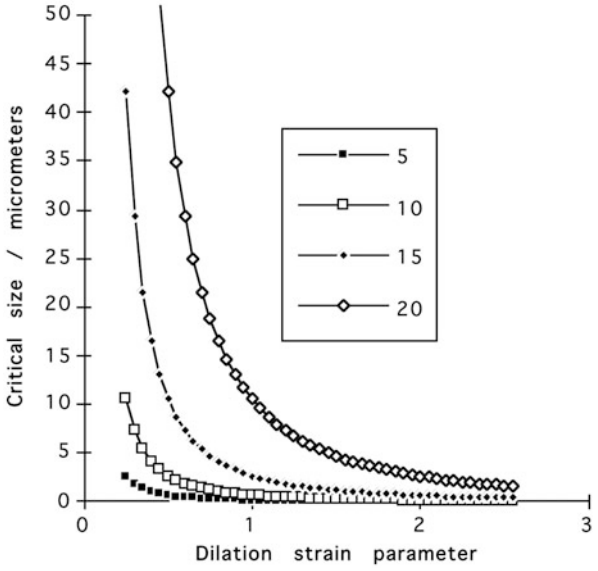

Fig. 20.15 Variation of the critical particle size as a function of the dilation strain for several values of the fracture toughness of the phase in tension. After [40]

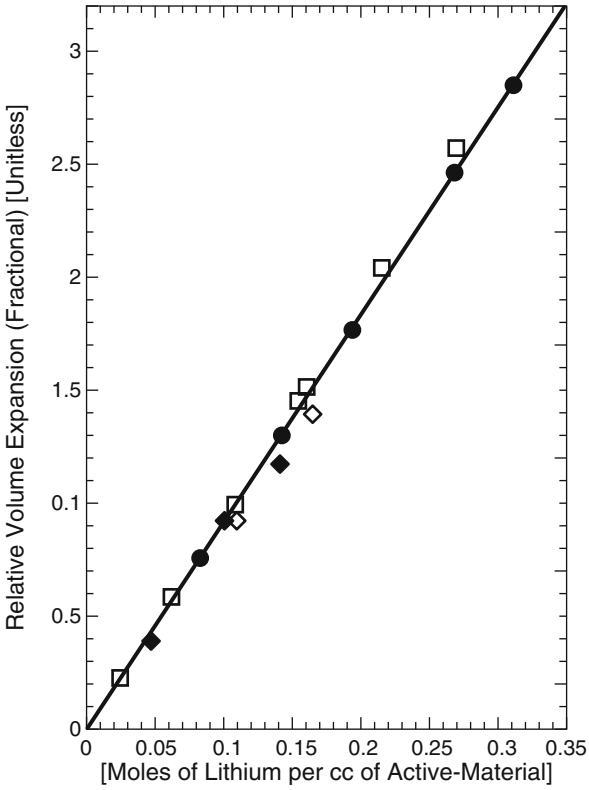

Fig. 20.16 Relation between volume expansion and the amount of lithium introduced into lithium alloys. After [41]

20.5.7 Modification of the Micro- and Nano-Structure of the Electrode

Some innovated approaches have been employed to ameliorate the decrepitation problem due to the large volume changes inherent in the use of metal alloy and silicon negative electrodes in lithium systems. If that can be done, there is the possibility of a substantial improvement in the electrode capacity.

The general objective is to give the reactant particles room to "breathe," so that they do not impinge upon each other. However, this has to be done so that they are maintained in electrical contact with the current collector system. Thus they cannot be physically isolated.

One interesting direction involves the modification of the shape of the surface upon which thin films of active material are deposited [42]. When the reactant film is dense, the volume changes and related stresses parallel to the surface cause separation from the substrate and loss of electronic contact. But if the surface is rough, there are high spots and low spots that have different local values of current

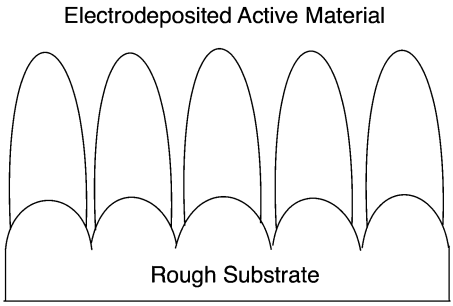

Fig. 20.17 Schematic drawing of the preferential deposition of reactant material upon protrusions on the substrate surface

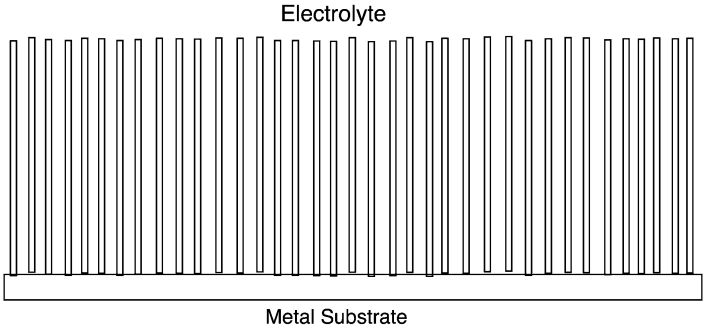

Fig. 20.18 Schematic drawing of electrode with a large number of nanowires

density when the active material is electrodeposited. The deposition rate is greater at the higher locations, and less elsewhere. The result is that the active material is mostly deposited at the high spot locations, and grows in a generally columnar shape away from the substrate. This leaves some space between the columnar growths to allow for their volume changes during operation of the electrode. This is illustrated schematically in Fig. 20.17.

Another alternative would be to make separated conductive spots on the surface, perhaps by the use of photolithography, that become the preferred locations for the deposition of reactant. By control of the spot arrangement, the electrodeposition can result in the formation of reactant material with limited impingement, thus allowing more *breathing room* when it undergoes charge and discharge.

It has been recently shown that a very attractive potential solution to this cycling problem is the use of reactant material in the form of nanowires. This is illustrated schematically in Fig. 20.18.

The particular example has been silicon [43]. Such wires can be grown directly upon a metallic substrate, so that they are all in good electronic contact. Because there is some space between the individual wires, they can expand and contract as lithium is added or deleted without the constraints present in either thin film or powdered electrode structures. Experiments showed that such fine wires can attain essentially the theoretical capacity of the Li–Si system.

20.5.8 Formation of Amorphous Products at Ambient Temperatures

This chapter has been primarily concerned with understanding the behavior of negative electrode materials under equilibrium or near-equilibrium conditions, from which the potential and capacity limits can be determined. Actual behavior in real applications always deviates from these limiting values, of course.

It was mentioned in earlier that repeated cycling can cause crystalline materials to become amorphous. The spectrum of materials in which amorphous phases have been formed under these conditions is now quite broad, and includes some materials of potential interest as positive electrode reactants, such as some vanadium-based materials with the general formula RVO_4, which R is Al, Cr, Fe, In, or Y [44].

There have been a number of observations that the operation of negative electrode materials at very high lithium activities can result in the formation of amorphous, rather than crystalline, products. The properties of these amorphous materials are different from those of the corresponding crystalline materials. This is very different from the amorphization of positive electrode materials under cycling conditions.

One example is a group of nitride alloys with structures related to that of Li_3N, which is known to be a fast ionic conductor for lithium, but in which some of the lithium is replaced by a transition metal, such as Co, have been found to become amorphous upon the first insertion of lithium [45–48].

Experimental evidence for the electrochemical amorphization of alloys in the Li–Si, Li–Sn, or Li–Ag systems was presented by Limthongkul [49]. In the latter two cases, this was only a transient phenomenon.

Especially interesting, however, have been experiments that gave evidence for the formation of amorphous silicon during the initial lithiation of a number of silicon-containing precursors, including SiB_3, SiO, $CaSi_2$, and $NiSi_2$ [50–52]. The electrochemical behavior of these materials after the initial lithiation cycle was essentially the same as that found in Si powder that was initially amorphous. There was, however, an appreciable amount of irreversible capacity in the first cycles of these precursors, about 1 mol of Li in the case of SiB_3 and the disilicides, which was evidently due to an irreversible displacement reaction with Li to form one mol of amorphous silicon. In the case of SiO the irreversible capacity amounted to about two mols of Li, which was surely related to the irreversible formation of Li_2O as well as the amorphous silicon.

Some of these materials with amorphous Si are of considerable potential interest as negative electrode reactants in lithium systems, as their charge/discharge curves are in an attractive potential range, they have reasonable kinetics, and their reversible capacities are quite high. The materials with silicon nanowire structure appear to be particularly attractive.

20.6 Protected Lithium Aqueous Electrolyte Systems

20.6.1 Introduction

As can be seen from the discussion thus far in this chapter, the attainment of two major advantages of the use of lithium negative electrodes, the production of electrochemical cells with large voltages and low weight, has involved the use of organic electrolytes. The stability range of aqueous electrolytes is limited by the decomposition of water.

There is another alternative, however, the use of "protected electrodes." This approach has been developed by the firm PolyPlus Battery Co., and involves the use of thin solid electrolyte ion-permeable membranes to separate lithium metal or alloy electrodes from an adjacent aqueous electrolyte. This concept was first publically presented in 2004 [53–55], and is currently being developed for production.

By the use of these solid electrolyte membranes in series with an aqueous electrolyte it is possible to make lithium-based aqueous batteries with output voltages considerably higher than is possible with an aqueous electrolyte alone.

This general scheme involves surrounding the lithium metal negative electrode reactant by a protective 20–50 μm thick lithium-conducting solid electrolyte membrane, and a gel electrolyte interlayer. This membrane is made of a version of "Lisicon," $Li_{1.3}Al_{0.3}Ti_{1.7}(PO_4)_3$, which has an ionic conductivity of 7×10^{-4} S/cm at 25 °C. This is illustrated schematically in Fig. 20.19.

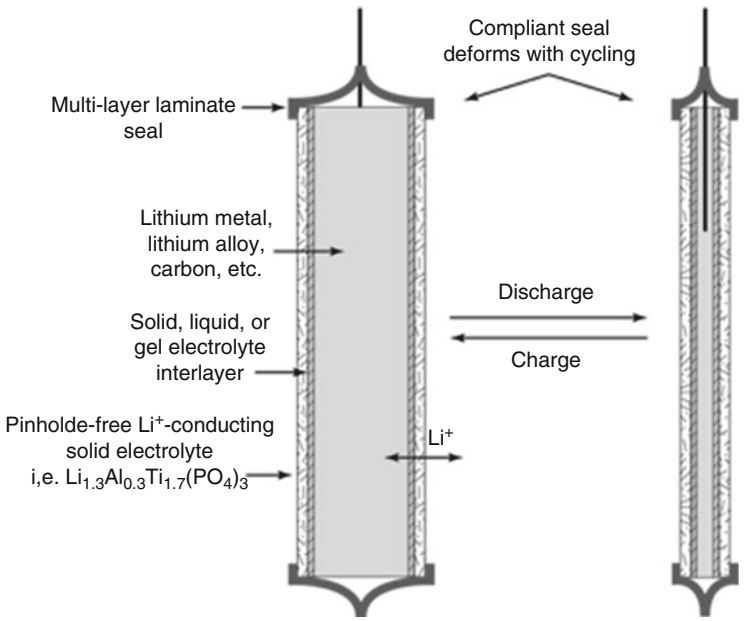

Fig. 20.19 Schematic representation of the PolyPlus cell configuration. After [55]

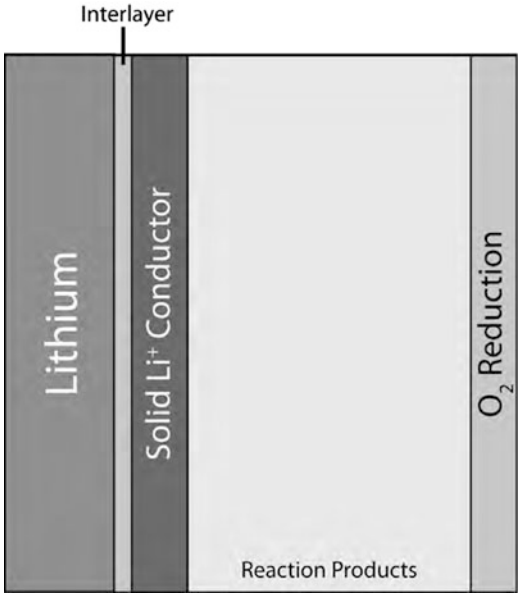

Fig. 20.20 General configuration of protected lithium. After [55]

Since the volume of the enclosed lithium changes during charging or discharging of such an electrode, the electrode shrinks, and the external seal must remain protective as the volume of the contained lithium varies. This is accomplished by the use of a flexible laminate seal material.

The theoretical specific energy of this configuration is high, about 10,000 Wh/kg, assuming that all of the lithium present can be used.

This type of configuration can be employed with several types of lithium-based batteries, Li–water primary cells, primary and secondary Li–air cells, and rechargeable Li–S systems.

The general configuration is illustrated in Fig. 20.20.

As an example, discharge curves at three different current densities for cells with protected lithium metal electrodes in a neutral aqueous electrolyte are shown in Fig. 20.21.

If there were no barrier layer separating them, lithium would react with water to form LiOH and hydrogen.

By protecting the lithium from water, the reaction product of lithium and air is lithium peroxide, Li_2O_2,

$$Li + O_2 = Li_2O_2 \tag{20.1}$$

From the Gibbs free energy of formation of Li_2O_2, it is found that this occurs at a potential of 2.96 V vs. Li in a nonaqueous solvent. The associated specific energy is 3,450 Wh/kg.

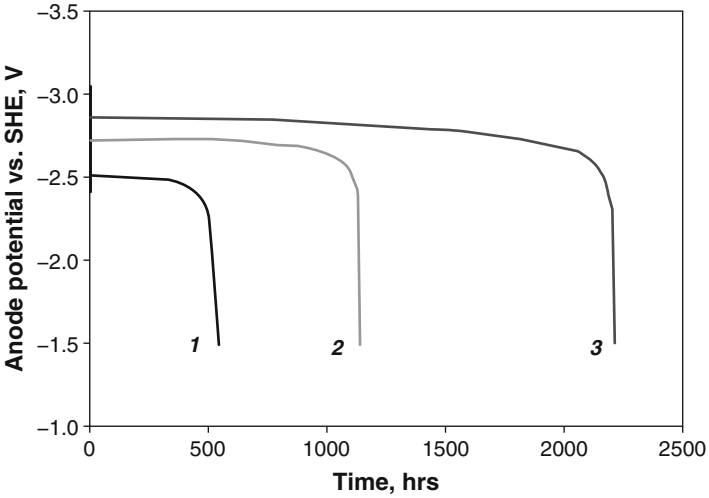

Fig. 20.21 Discharge curves of protected lithium electrodes at several current densities: (*1*) 2.0 mA/cm^2, (*2*) 1.0 mA/cm^2, (*3*) 0.5 mA/cm^2 [55]

However, in an aqueous solvent the reaction product is LiOH, from

$$4\,\mathrm{Li} + \mathrm{O_2} + 2\mathrm{H_2O} = 4\mathrm{LiOH} \tag{20.2}$$

which occurs at a potential of 3.45 V vs. Li. The associated specific energy in this case is 3,850 Wh/kg.

References

1. Huggins RA, Elwell D (1977) J Cryst Growth 37:159
2. Wagner C (1954) J Electrochem Soc 101:225
3. Wagner C (1956) J Electrochem Soc 103:571
4. Deublein, Huggins RA (1986) Solid State Ionics. 18/19: 1110
5. von Sacken U, Nodwell E, Dahn JR (1994) Solid State Ionics 69:284
6. Winter M, Moeller K-C, Besenhard JO (2004) In: Nazri G-A, Pistoia G (eds) Lithium Batteries, Science and Technology. Kluwer Academic. p 144
7. Dahn JR, Sleigh AK, Shi H, Way BM, Weydanz WJ, Reimers JN, Zhong Q, von Sacken U (1994) In: Pistoia G (ed) Lithium Batteries. Elsevier. p 1
8. Fredenhagen K, Cadenbach G (1926) Z Anorg Allg Chem 158:249
9. Guerard D, Herold A (1975) Carbon. 13: 337
10. Wertheim GK, Van Attekum P.M.Th.M, Basu S (1980) Solid State Communications. 33:1127
11. Ebert LB (1976) In: Huggins RA (ed) Annual Review of Materials Science, vol. 6. Annual Reviews Inc. p 181
12. Besenhard JO, Fritz HP (1974) J Electroanal Chem 53:329
13. Yazami R, Touzain P (1983) J Power Sources 9:365
14. Basu S (1981) US Patent No 4,304,825, Dec 8 1981

15. Basu S (1983) US Patent No 4,423,125, Dec 27 1983
16. Nagaura T, Tozawa K (1990) Progress in Batteries and Solar Cells. JEC. 9: 209
17. Nagaura T (1991) Progress in Batteries and Solar Cells. JEC 10: 218
18. Franklin RE (1951) Proc Roy Soc (London) A209: 196
19. Yazami R. Personal Communication
20. Daumas N, Herold A (1969) CR Acad Sci C 286:373
21. Zheng T, Liu Y, Fuller EW, Tseng S, von Sacken U, Dahn JR (1995) J Electrochem Soc 142:2581
22. Zheng T, Xue JS, Dahn JR (1996) Chem Mat 8:389
23. Zheng T, McKinnon WR, Dahn JR (1996) J Electrochem Soc 143:2137
24. Yao NP, Heredy LA, Saunders RC (1971) J Electrochem Soc 118: 1039
25. Gay EC et al (1976) J Electrochem Soc 123:1591
26. Lai SC (1976) J Electrochem Soc 123:1196
27. Sharma RA, Seefurth RN (1976) J Electrochem Soc 123:1763
28. Seefurth RN, Sharma RA (1977) J Electrochem Soc 124:1207
29. Ogawa H (1984) Proceedings of 2nd International Meeting on Lithium Batteries. Elsevier Sequoia, Lausanne, p 259
30. Wang J, King P, Huggins RA (1986) Solid State Ionics 20:185
31. Wang J, Raistrick ID, Huggins RA (1986) J Electrochem Soc 133:457
32. Boukamp BA, Lesh GC, Huggins RA (1981) J Electrochem Soc 128:725
33. Boukamp BA, Lesh GC, Huggins RA (1981) In: Venkatasetty HV (ed) Proc. Symp. on Lithium Batteries. Electrochem Soc, p 467
34. Huggins RA, Boukamp BA. US Patent 4,436,796
35. Anani A, Crouch-Baker S Huggins RA (1987) In: Dey AN (ed) Proc. Symp. on Lithium Batteries. Electrochem Soc, p 382
36. Anani A, Crouch-Baker S, Huggins RA (1988) J Electrochem Soc 135:2103
37. Wen CJ, Huggins RA (1980) J Solid State Chem 35:376
38. Wen CJ, Huggins RA (1981) J Electrochem Soc 128:1181
39. Yang J, Winter M, Besenhard JO (1996) Solid State Ionics 90:281
40. Huggins RA, Nix WD (2000) Ionics 6:57
41. Timmons A (2007) PhD Dissertation. Dalhousie University
42. Fujimoto M, Fujitani S, Shima M et al. (2007) US Patent 7,195,842. March 27, 2007
43. Chan CK, Peng H, Liu G, McIlwrath K, Feng Zhang X, Huggins RA, Cui Y (2008) Nat Nanotechnol 3:31
44. Piffard Y, Leroux F, Guyomard D, Mansot J-L, Tournoux M (1997) J Power Sources 68:698
45. Nishijima M, Kagohashi T, Imanishi N, Takeda Y, Yamamoto O, Kondo S (1996) Solid State Ionics 83:107
46. Shodai T, Okada S, Tobishima S-i, Yamaki J-i (1996) Solid State Ionics 86–88:785
47. Nishijima M, Kagohashi T, Takeda Y, Imanishi N, Yamamoto O (1996) 8th International Meeting on Lithium Batteries. p 402
48. Shodai T, Okada S, Tobishima S, Yamaki J (1996) 8th International Meeting on Lithium Batteries. p 404
49. Limthongkul P (2002) PhD Thesis. Mass. Inst. of Tech
50. Klausnitzer B (2000) PhD Thesis. University of Ulm
51. Netz A (2001) PhD Thesis. University of Kiel
52. Netz A, Huggins RA, Weppner W (2002) Presented at 11th International Meeting on Lithium Batteries. Abstract No. 47
53. Visco SJ, Nimon E, Katz B, De Jonghe LC, Chu M-Y (2004) 12th International Meeting on Lithium Batteries, Nara, Japan, June 2004
54. Visco SJ, Nimon E, Katz B, Chu M-Y, De Jonghe LC (2009) Scalable Energy Storage: Beyond Li-Ion. Almaden Inst., San Jose, CA, August 2009
55. Visco SJ, Nimon E, Nimon VY, Katz B, Chu M-Y, De Jonghe LC (2015) International battery Association and Pacific Power Source Symposium. Hilton Waikoloa Village, Hawaii, Jan 2015